

Supplementary Information

Nickel molecular catalyst grafted graphene quantum dots on porous NiO as a photocathode for H₂ evolution under visible light

Wenbo Su, Yue Zhu, Xin Su, Nanjun Huang, Xiaoshuang Yin, Ying Liu, Wenzhong Yang and Yun Chen^{†*}

[†] School of Chemistry and Molecular Engineering, Nanjing Tech University, No. 30 Puzhu Road (S), Nanjing 211816, China

* Corresponding author.

E-mail: ychen@njtech.edu.cn (Y. Chen)

1. Chemical materials

Nickel (II) nitrate hexahydrate (AR), ethylene glycol (AR), glucose (AR), N,N-dimethylformamide were purchased from Sinopharm Chemical Reagent Co., Ltd.; APTES (aminopropyltriethoxysilane) (99%), CX-72 carbon black (99%) were purchased from Shanghai Macklin Biochemical Co., Ltd.; Nitric acid (68%), methanol (99.5%), potassium hydroxide (99.5%), ammonia (25%~28%), chloroform (99%), ethanol (95%) and dichloromethane (99.5%) were purchased from Shanghai Lingfeng Chemical Reagent Co., Ltd.; 2-acetylpyridine (98%), 4-bromobenzaldehyde boron (97%), (4-formylphenyl) boronic acid (97%), tetrakis(triphenylphosphine)palladium (Pd>9.0%), nickel chloride (AR) and diethylenetriamine (99%) were purchased from Sigma-Aldrich and used as received without further purification. The ultrapure water with 18.2 MΩ cm (HITECH, Medium-E400, China) was used in the experiments.

2. Characterization

The UV-Vis absorption measurements were carried out on an Agilent 8453 spectrophotometer. The Fluorescence spectra were taken on Edinburgh FS5. High-resolution transmission electron microscopy (HRTEM) was performed by JEOL-2100F operated at an accelerating voltage of 200 kV. Field emission scanning electron microscopy (FESEM) images were recorded on a JSM-7600F (JEOL) with an accelerating voltage of 15 kV. X-Ray diffraction (XRD) measurements were performed on a Bruker D8 Advance under Cu-K α radiation ($\lambda = 1.54056 \text{ \AA}$). The chemistry state of elements was evaluated by X-Ray photoelectron spectroscopy instrument (XPS) using Thermo ESCALAB 250xi spectrophotometer with Al-K α radiation. The binding energy scale was calibrated using the C 1s peak at 284.6 eV. The Fourier Transform infrared (FT-IR) spectroscopy was obtained with a Thermo Nicolet. Gas chromatography (GC) was performed by Fuli GC9790P using a 5 \AA molecular sieve column and thermal conductivity detector.

3. Electrocatalytic experiments

All electrochemical experiments were performed with a CHI660E Electrochemical Workstation. Linear sweep voltammogram (LSV) of the as-prepared photocathodes were carried out in 0.1 M phosphate buffer solution at pH 6.8 in a two-compartment cell, using platinum counter electrode and Ag/AgCl in 3 M KCl as the reference electrode. The scan rate of LSV tests was 100 mV s⁻¹. Before measurement, the testing solution (20 mL) was degassed for at least 20 min by flushing high purity

nitrogen. For photocurrent measurement, the photocathode was illuminated under a 100 W Xe-lamp. All potentials were converted to the NHE reference using $E(\text{NHE}) = E(\text{Ag}/\text{AgCl}) + 0.197 \text{ V}$.

4. Synthesis of GQDs

GQDs were prepared to refer to literature with some modifications¹. In brief, 0.2 g dried CX-72 carbon black was put into 50 mL 6 M HNO_3 followed by refluxing at 135 °C for 24 h. After cooling to room temperature, the suspension was centrifuged for 10 min to obtain a supernatant (7500 r/min). Then, the supernatant was heated at 140 °C to evaporate the water and HNO_3 , and a reddish-brown solid was obtained. The GQDs were dissolved in an aqueous solution and sonicated for 10 min. The solution was ultrafiltered through a microporous membrane with 0.22 μm .

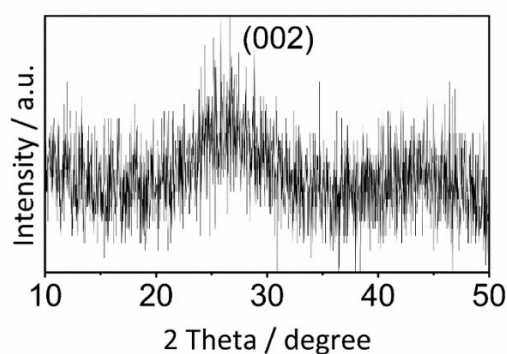


Fig. S1 XRD patterns of GQDs.

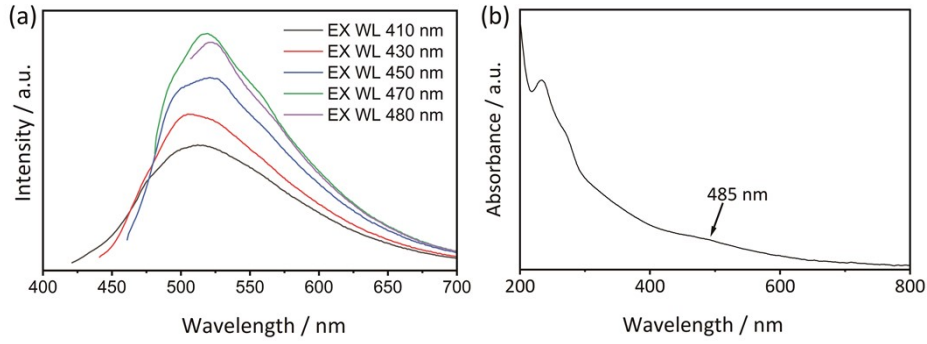


Fig. S2 (a) Fluorescence emission intensities of the GQDs at different excitation wavelengths. (b) UV-Vis absorption spectrum of GQDs.

The band gap and valence band of GQDs

The band gap (ΔE_g) of GQDs could be calculated from the first excitation absorption peak of GQDs (λ_{peak}) using equation (1)²:

$$\Delta E_g = \frac{1240}{\lambda} (1)$$

In our experiments, the band-edge emission (λ_{peak}) of the GQDs was 485 nm. Thus, ΔE_g was determined as 2.5 eV.

5. Preparation of NiO film electrode

The FTO substrate (1 cm × 2 cm) was carefully cleaned by ultrasonication sequentially in soap water, ethanol and acetone for 20 min successively. Next, the substrate was placed into a Teflon-lined stainless-steel autoclave. NiO porous film electrode was fabricated following the reported method³. Firstly, 5 mmol $\text{Ni}(\text{NO}_3)_2 \cdot 6\text{H}_2\text{O}$ was dissolved in 25 mL ultrapure water and 25 mL ethylene glycol to form a light green solution. Subsequently, 0.05 mmol glucose was added into the solution and stirred for 30 min. The aqueous solution was maintained at 170 °C for 24 h and allowed to cool down to room temperature naturally. The light green substrate

was washed with deionized water and ethanol 5 times each, and it dried at 60 °C for 14 h. The deposited NiO film on the non-conductive side was removed with water flow during the washing process. Finally, the sample was annealed in a muffle furnace at 350 °C for 3 h in air. For preparation of APTES-NiO film electrode, The NiO-FTO electrode was immersed in 0.2 wt % 3-aminopropyltriethoxysilane (APTES) toluene solution at room temperature for 10 min. Then, the electrode was removed, washed with toluene, and heated at 110 °C for 2 h ⁴.

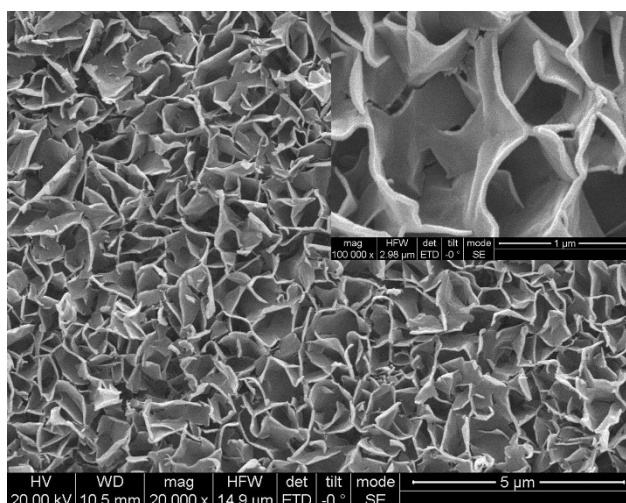


Fig. S3 FESEM image of porous NiO films on FTO glass substrate.

6. Preparation of $[(\text{tpy-CH=N})_2\text{Ni}]\text{Cl}_2$

$[(\text{tpy-CH=N})_2\text{Ni}]\text{Cl}_2$ was prepared by literature procedures. The synthetic route for $[(\text{tpy-CH=N})_2\text{Ni}]\text{Cl}_2$ was shown in Fig. S4 ⁵ :

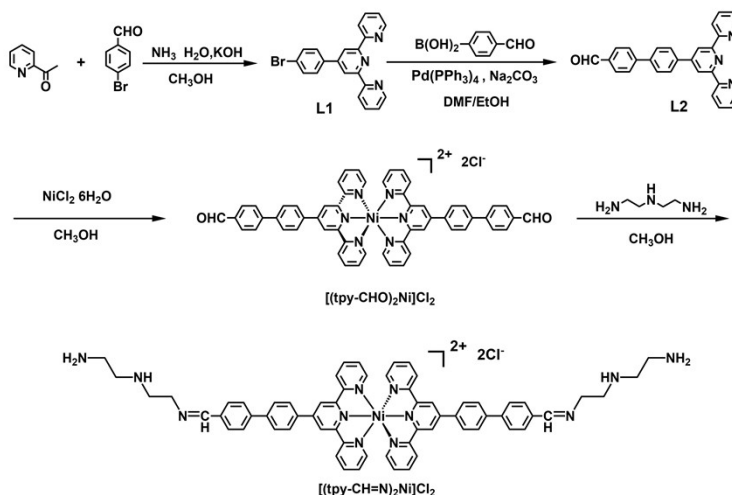


Fig. S4 Synthesis of complex $[(\text{tpy-CH=N})_2\text{Ni}]\text{Cl}_2$.

Firstly, 60 mmol 2-acetylpyridine and 30 mmol 4-bromobenzaldehyde were dissolved in 100 mL methanol. Add 20 mL KOH (15 wt%) and 1.4 mL $\text{NH}_3 \cdot \text{H}_2\text{O}$ (25~28%) into the solution and stirring vigorously for 3 days at room temperature. The formed precipitate was filtered and washed with ultrapure water until it was found to be free of any base. The precipitate was dissolved in CHCl_3 , washed with dilute NaHCO_3 , dried with MgSO_4 and evaporated to give a solid. Recrystallization from absolute ethanol gave pure L1. $^1\text{H NMR}$ (400 MHz, CDCl_3) δ 8.71 (m, 2H), 8.68 (d, $J = 4.8$ Hz, 2H), 8.65 (d, $J = 8.0$ Hz, 2H), 7.87 (td, $J = 7.7, 1.7$ Hz, 2H), 7.77 (m, 2H), 7.63 (d, $J = 8.5$ Hz, 2H), 7.36 (m, 2H).

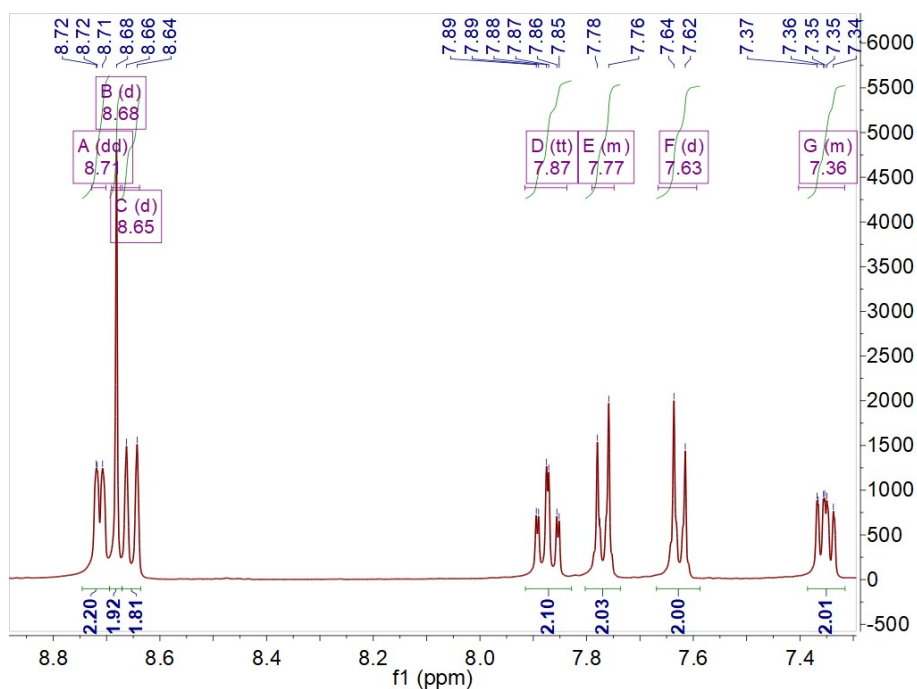


Fig. S5 The ^1H NMR characterization for Compound L1.

The next, 10 mmol L1, 10 mmol (4-formylphenyl) boronic acid, 0.1 mmol $\text{Pd}(\text{PPh}_3)_4$, 80 mmol Na_2CO_3 , 60 mL DMF and 40 mL ethanol were held at 100 °C under N_2 atmosphere for 8 h. The reaction mixture was cooled to room temperature and 100 mL water was added. The mixture was extracted three times with CH_2Cl_2 and the organic extracts were dried by MgSO_4 , filtered and concentrated in vacuo. Purification by column chromatography gave L2. ^1H NMR (400 MHz, CDCl_3) δ 10.07 (s, 1H), 8.78 (s, 2H), 8.74 (ddd, $J = 10.1, 5.5, 4.7$ Hz, 2H), 8.68 (d, $J = 7.9$ Hz, 2H), 7.99 (dd, $J = 17.4, 8.3$ Hz, 4H), 7.89 (td, $J = 7.7, 1.8$ Hz, 2H), 7.79 (dd, $J = 18.4, 8.3$ Hz, 4H), 7.36 (ddd, $J = 7.4, 4.8, 1.1$ Hz, 2H).

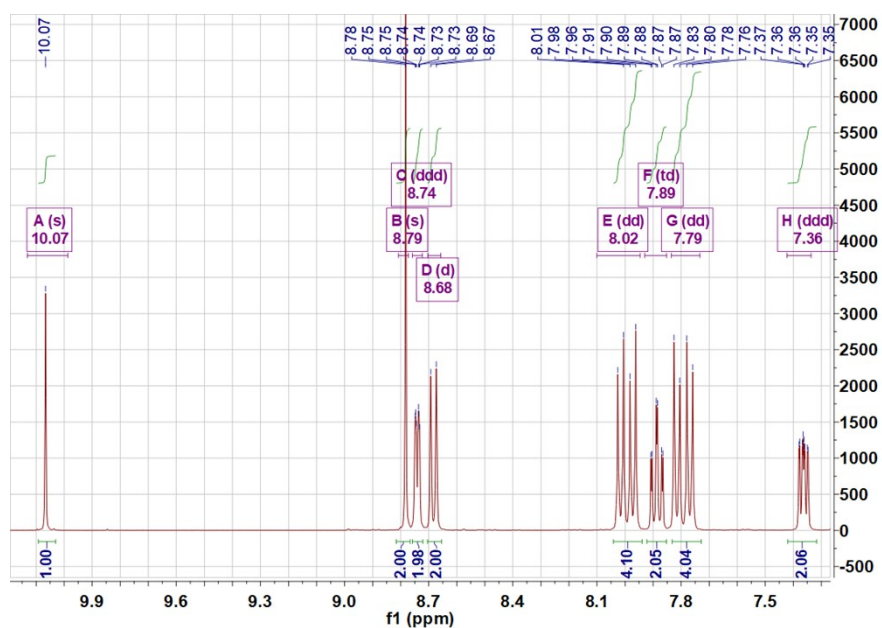


Fig. S6 The ^1H NMR characterization for Compound L2.

Afterwards, 1.2 mmol L2 and 0.6 mmol $\text{NiCl}_2 \cdot 6\text{H}_2\text{O}$ were added to 50 mL methanol and refluxed at 65 °C for 10 h. After cooling to room temperature, the solid was collected by filtration and recrystallized from methanol to give $[(\text{tpy-CHO})_2\text{Ni}]\text{Cl}_2$. 0.5 mmol $[(\text{tpy-CHO})_2\text{Ni}]\text{Cl}_2$ was dissolved in 50 mL methanol to form a homogeneous solution. Then, 0.5 mmol Ethylene Diamine Tetraacetic Acid was added dropwise and the solution was refluxed at 65 °C for 10 h. After cooling to room temperature, the products $[(\text{tpy-CH=N})_2\text{Ni}]\text{Cl}_2$ were collected by concentration under reduced pressure. The analysis of the mass spectra showed that $[\text{M}-2\text{Cl}+\text{H}]^+=1054.2965$ was in good consistent with the theoretical value of $[\text{M}-2\text{Cl}+\text{H}]^+=1054.4417$ ⁵.

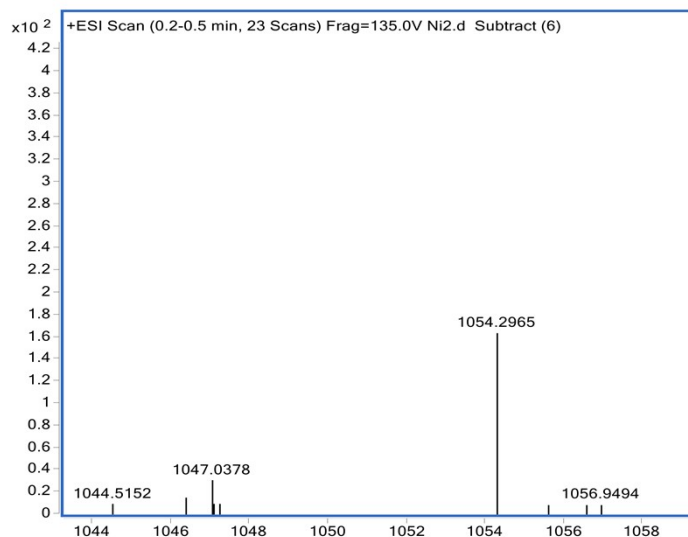


Fig. S7 High resolution mass spectrometry of $[(\text{tpy-CH=N})_2\text{Ni}]\text{Cl}_2$.

7. Fabrication of the photocathode

The NiO film electrode with 1 cm^2 active area was soaked into GQDs solution at ambient temperature for 24 h. Then it was washed with ultrapure water and dried at room temperature. $[(\text{tpy-CH=N})_2\text{Ni}]\text{Cl}_2$ (NiN) was loaded on the surface of GQDs sensitized NiO electrode by dropping its acetonitrile solution (1 mM) of different volumes (75 μL , 100 μL , 125 μL , and 150 μL) with 5% Nafion, followed by drying under air flow.

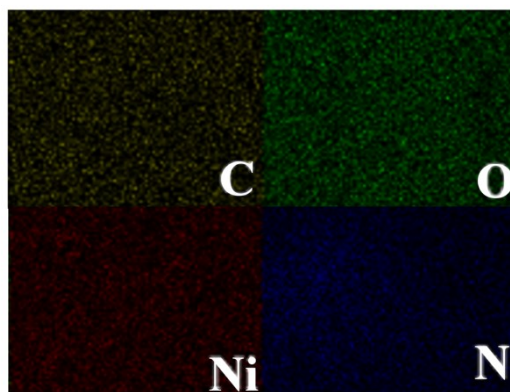


Fig. S8 The elemental mapping of NiN-GQDs-NiO photocathode by EDX spectroscopy.

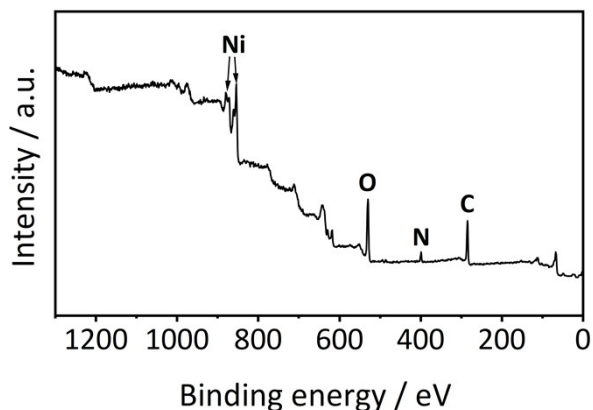


Fig. S9 XPS scan spectrum of NiN-GQDs-NiO photocathode at 0-1200 eV.

In order to optimize the deposition amount of GQDs, the soaking time of NiO/FTO in GQDs solution (1 mg mL^{-1}) was changed from 1 to 5 h. The results showed in Fig. S10a that soaking 3 h can maximize the photocurrent density of GQDs-NiO photocathode. Since the surface of GQDs contained a large amount of carboxyl groups, it can be condensed with the amino group of NiN.

Fig. S10b showed when the deposition amount of NiN increased, the photocurrent density gradually enhanced as well. And when the deposition amount of Ni catalyst was $75 \mu\text{L}$, the current density reached the highest amount. The deposition of excess quantum dots and co-catalysts hampered the charge transfer, which caused the drop in photocurrent gradually.

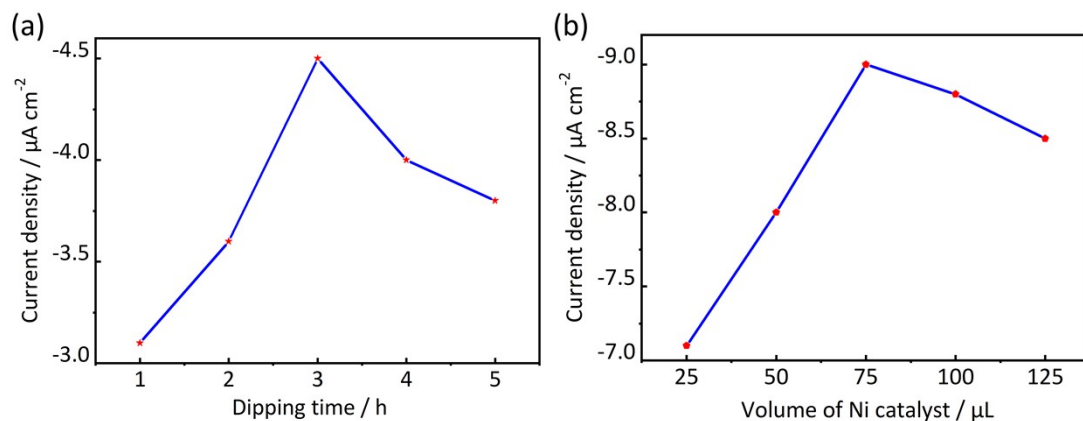


Fig. S10 (a) Photocurrent density of the GQDs-NiO electrodes with different dipping times. (b) Photocurrent density of the NiN-GQDs-NiO electrode with different NiN co-catalyst loadings.

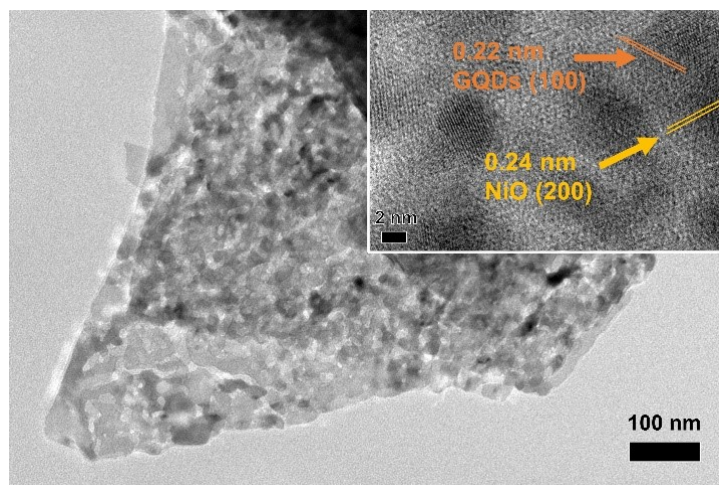


Fig. S11 The HRTEM image of the assembled NiN-GQDs-NiO photocathode after photoelectric testing.

The HRTEM of the NiN-GQDs-NiO photoelectrode after photovoltaic testing was shown in Figure.S11. It showed that the GQDs were still very stable on the surface of NiO without aggregation. The surface of NiO was modified with 3-aminopropyltriethoxysilane (ATPES), which was rich in amino groups. Therefore, carboxyl functionalized GQDs were covalently bonded on the NiO surface via amido bonds. It achieved the excellent coupling for great stability and dispersibility⁴.

Notes and References

1. Y. Dong, C. Chen, X. Zheng, L. Gao, Z. Cui, H. Yang, C. Guo, Y. Chi and C. M. Li, *Journal of Materials Chemistry*, 2012, **22**, 8764-8766.
2. A. Kudo and Y. Miseki, *Chemical Society Reviews*, 2009, **38**, 253-278.
3. Y. Zhang and Z. Guo, *Chemical Communications*, 2014, **50**, 3443-3446.
4. C. X. Guo, Y. Dong, H. B. Yang and C. M. Li, *Advanced Energy Materials*, 2013, **3**, 997-1003.
5. W. Zhao, Y. Huang, Y. Liu, L. Cao, F. Zhang, Y. Guo and B. Zhang, *Chemistry – A European Journal*, 2016, **22**, 15049-15057.